



ELSEVIER

Solid State Ionics 101–103 (1997) 451–455

**SOLID  
STATE  
IONICS**

# Theory of diffusion-controlled colloid formation in irradiated solids

V.N. Kuzovkov<sup>a,b,\*</sup>, E.A. Kotomin<sup>a,c</sup><sup>a</sup>*Institute of Solid State Physics, 8 Kengaraga Str., Riga LV-1063, Latvia*<sup>b</sup>*Institut für Physikalische und Theoretische Chemie, Technische Universität Braunschweig, D-38106, Braunschweig, Germany*<sup>c</sup>*Fachbereich Physik, Freie Universität Berlin, Arnimallee 14, 14195 Berlin, Germany*

---

## Abstract

The kinetics of diffusion-controlled aggregation of Frenkel defects (interstitial atoms and vacancies) under irradiation of solids is studied on a microscopic level. The theory is based on the discrete-lattice formalism for the single defect densities (concentrations) and coupled joint densities of similar and dissimilar defects treated in terms of the Kirkwood superposition approximation. The physical model takes into account random defect creation, diffusion, attraction and bimolecular,  $A + B \rightarrow 0$  recombination. Conditions of the efficient aggregation of vacancies and interstitials are studied. The cooperative character of the aggregation process is shown.

PACS: 82.20.Mj; 05.40.+j; 61.46.+w; 61.72.J

Keywords: Frenkel defects; Alkali halides; Cluster; Defect formation; Diffusion; Nucleation

---

## 1. Introduction

As is well known, the primary radiation defects in ionic solids – the *F* centres (electron trapped by anion vacancy) and the *H* centres (interstitial halide atoms) – begin to aggregate under intensive irradiation and at temperatures high enough (typically above the room temperature, RT). This leads to the formation of alkali metal colloids and gas bubbles (see [1,2] and references therein); a similar process occurs also in heavily irradiated metals [3,4]. The intensive experimental studies of the conditions for defect aggregation and further colloid formation (such as the temperature interval, dose rate, etc.) continue nowadays for alkali halides [5,6] and

technologically important ceramics [7]. This problem is also interesting from the fundamental point of view, being an example of pattern formation and self-organization in reaction–diffusion systems far from equilibrium [8].

Existing theories of the radiation-induced defect aggregation and colloid formation could be classified, in terms of the mathematical formalism used, into three categories: macroscopic [9], mesoscopic [10–12] and microscopic [13]. The latter are first-principle theories using no fitting or uncertain parameters but only several basic defect parameters like diffusion constants and interaction potentials.

In the present paper, we briefly discuss the idea of the first microscopic discrete-lattice theory of diffusion-controlled aggregation during the bimolecular annihilation,  $A + B \rightarrow 0$ , under the permanent particles' source and present its results for the study of

---

\*Corresponding author. Fax: +371 711-2583; e-mail: kuzovkov@acad.latnet.lv

cooperative kinetics of colloid formation under prolonged irradiation of ionic solids.

## 2. The model

The physical model includes creation of the interstitials and vacancies (called hereafter just defects A and B), with the (dose) rate  $p$ , AB pairs are not spatially correlated at birth and recombine when during their migration they approach each other within the nearest-neighbour (NN) distance. Therefore, their macroscopic concentrations always coincide, i.e.  $C = C_A = C_B$ . Isolated (single) defects hopping with the activation energy  $E_\lambda$  are characterized by the diffusion coefficients  $D_\lambda = D_0 \exp(-E_\lambda / k_B T)$ ,  $\lambda = A, B$ . When several defects are closely spaced, the hop rate of a given defect to the nearest empty lattice site is determined by both the local defect configuration and the interaction between defects; this can change its effective diffusion coefficient  $D_\lambda^{\text{eff}}$  by many orders of magnitude compared to that for a single defect. It affects the effective reaction rate  $K$  of the A and B recombination.

As follows from previous theoretical studies [10–16], defect attraction plays a decisive role in the aggregation process, it is incorporated in our model via three types of the NN attractions between the two kinds of NN defects (in the spirit of the Ising model):  $E_{AA}$ ,  $E_{AB}$  and  $E_{BB}$ .

## 3. Correlation function formalism

The mathematical formalism and the relevant computer program Kinetica will be described in detail elsewhere [17]. It is a generalization of our previous microscopic many-point density approach [13,18–20] for the discrete lattice case which allows us to avoid the limitations of a continuum model, to increase the computation speed and thus to study the aggregation kinetics in the very wide time interval, exceeding ten orders of magnitude. The theory is an approximation for the three-particle densities [18,19] and thus operates with a set of coupled kinetic equations for the lattice defect densities (concentrations)  $C_\lambda(t)$ ,  $\lambda = 0, A, B$  and the joint correlation functions  $F_{\lambda\nu}(|\mathbf{r}_\lambda - \mathbf{r}_\nu|, t)$  where  $\mathbf{r}_\lambda$  and  $\mathbf{r}_\nu$  are coordinates of the two lattice sites and  $t$  is the time. The

simultaneous analysis of the joint correlation functions for similar (AA, BB) and dissimilar (AB) pairs, as well as for 0A, 0B pairs (empty site-defect) permit to study the spatio-temporal evolution of the strongly non-equilibrium system, in particular, in crystals with radiation defects [13,17–20].

It is also convenient to characterize the aggregation process by monitoring the concentrations of single defects  $C_\lambda(1)$  (no other defects in NN sites) and dimer defects  $C_\lambda(2)$  (two similar defects are NN). Finally, large aggregates could be characterized by the integral values of the number of particles  $N_\lambda$ ,  $N_B$  therein and their sizes (radii)  $R_A$  and  $R_B$ .

## 4. Results

### 4.1. Concentration growth

Let us now study the kinetics of colloid growth at two different temperatures – 300 K (room temperature, RT) and 500 K (high temperature) – in a model-like alkali halide crystal; its typical parameters are given in the caption to Fig. 1. The first conclusion from Fig. 1 is that at both temperatures starting from the very short times,  $t \ll 1$  s, most interstitials are already aggregated; the concentrations of single and dimer interstitials,  $C_A(1)$  and  $C_A(2)$ , are about 10 orders of magnitude less than the macroscopic (total) concentration  $C = C_A = 10^{-10}$ , i.e. most of the interstitials belong to larger aggregates. This is a direct result of high mobility of interstitials A (the activation energy for hopping is only 0.1 eV) even when moderate mutual attraction leads to the formation of large aggregates. In contrast, slowly mobile vacancies B ( $E_B = 0.9$  eV) exist for a much longer times predominantly as single defects – up to some characteristic time  $t_0$ . This time  $t_0$  greatly depends on the temperature and decreases from  $10^4$  s at RT down to  $10^{-2}$  s at 500 K, i.e. by six orders of magnitude. As  $t > t_0$ , the concentration of single and dimer defects becomes similar, and at longer times we observe the growth of more complex aggregates (trimers, etc.).

### 4.2. Aggregate characterization

Below the critical time  $t_0$  mean number of interstitials in the A-aggregate is practically constant at both

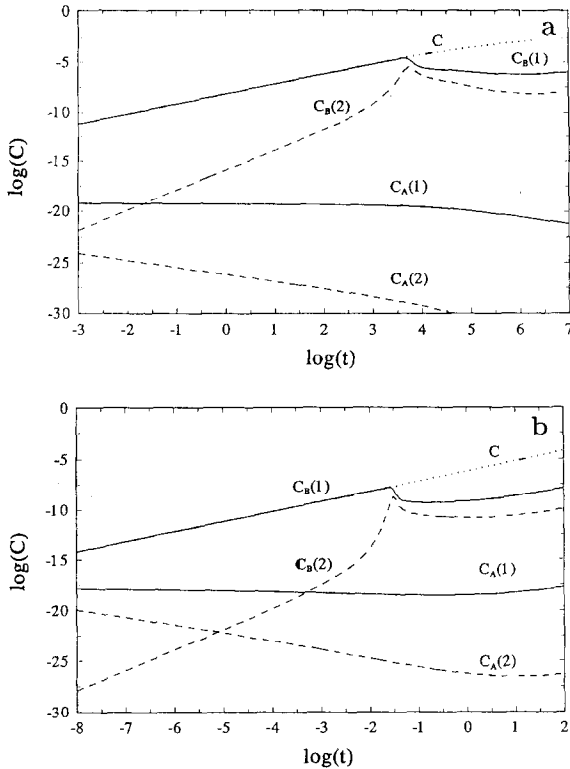


Fig. 1. The time development of defect concentrations of interstitials (A) and vacancies (B) at 300 K (a) and 500 K (b).  $C$  are macroscopic concentrations whereas  $C_A(1)$  and  $C_A(2)$ ,  $\lambda = A, B$  are single defect and dimer defect concentrations respectively. Concentrations are in dimensionless units ( $n\lambda a_0^3$ ), time ( $t$ ) in seconds, the dose rate (irradiation intensity)  $p = 10^{14} \text{ cm}^{-3} \text{ s}^{-1}$ . The migration and attraction energies are chosen to be typical for alkali halide crystals:  $E_A = 0.1 \text{ eV}$ ,  $E_B = 0.9 \text{ eV}$ ,  $E_{AA} = -0.2 \text{ eV}$ ,  $E_{AB} = -0.2 \text{ eV}$ ,  $E_{BB} = -0.1 \text{ eV}$ .  $D_0 = 10^{-3} \text{ cm}^2 \text{ s}^{-1}$  [9–11,13].

temperatures studied,  $N_A \approx 15$ , whereas  $N_B \approx 1$  (single vacancies dominate). However, as soon as  $N_B$  shows a sharp increase at  $t > t_0$ ,  $N_A$  does too. That is, the aggregation of vacancies greatly enhances that of interstitials – we observe the cooperative process of the simultaneous aggregation of the two kinds of defects.

This conclusion is supported by similar behaviour of the size of these two kinds of aggregates. The physical background of this effect is clear: at  $t > t_0$  most of interstitials are already aggregated and their further growth is restricted by the recombination with slowly mobile single vacancies. When the latter begin to aggregate too, they no longer control the behaviour (and prevent additional aggregation) of the

interstitials. As a result, we have a positive back-coupling of the two kinds of aggregation processes, mentioned above as the cooperative effect. At higher temperature and  $t > t_0$  the aggregate size is much larger.

### 4.3. Conditions for colloid formation

A very interesting condition of the cooperative aggregation of interstitials and vacancies could be learnt from Fig. 2. At  $t < t_0$  the effective diffusion coefficient of vacancies,  $D_B^{\text{eff}}$ , practically coincides with that for single vacancies,  $D_B$ , whereas that for the interstitials,  $D_A^{\text{eff}}$  dramatically decreases with time by many orders of magnitude due to effective interstitial aggregation. This continues up to the moment  $t_0$  when  $D_A^{\text{eff}}$  in magnitude becomes close to the small diffusion coefficient of single vacancies,  $D_B \approx 10^{-21} \text{ cm}^2 \text{ s}^{-1}$ . Only after the mobilities of the two kinds of defects become comparable,  $D_A^{\text{eff}}$  is stabilized but in its turn,  $D_B^{\text{eff}}$  begins to decrease, thus indicating the effective aggregation of vacancies. The broken line in Fig. 2 shows that the effective reaction rate  $K$  decreases also by many orders of magnitude, being well correlated to the  $D_A^{\text{eff}}$  behaviour.

### 4.4. Spatial distribution of defects

The relative spatial distribution of defects at the late stage of aggregation is seen in Fig. 3. Large magnitudes of the joint correlation functions of

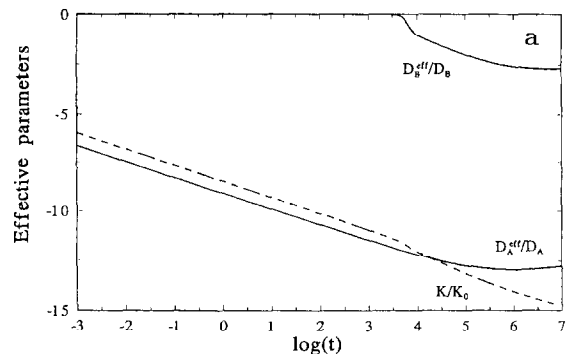


Fig. 2. Time development of the relative effective coefficients  $D_A^{\text{eff}}$ ,  $\lambda = A, B$  of interstitials A and vacancies B and the relative recombination rate  $K$  at 300 K.

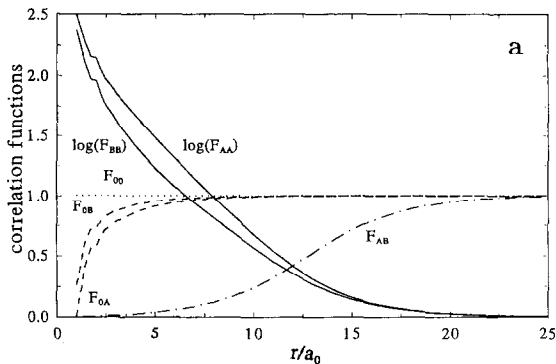


Fig. 3. The joint correlation functions at 300 K for large times is plotted as a function of the relative distance between the particles, see explanation in the text. Note that  $F_{AA}$  and  $F_{BB}$  are plotted in the semi-logarithmic scale.

similar defects,  $F_{AA}$ ,  $F_{BB}$ , at short relative distances clearly demonstrate the strong aggregation of both interstitials and vacancies. At RT the relative distance of  $r \approx 15a_0$  the correlation functions approach the asymptotic value of unity. This value of  $r$  is a qualitative estimate of the radius of the aggregates.

Another important conclusion is suggested from this figure: despite very different mobilities and interaction energies of interstitials and vacancies, the cooperative effects in their aggregation lead to quite similar final aggregates observed at the end of irradiation.

The correlation function for the dissimilar defects,  $F_{AB}(r)$ , is anti-correlated to  $F_{AA}$ ,  $F_{BB}$ , i.e. it increases at RT from almost zero at  $r \leq 7a_0$  up to unity at  $r \approx 15\text{--}20a_0$ , which gives us an estimate of the average distance between aggregates of dissimilar particles (defects). Finally, the joint correlation functions 'empty site-defect',  $F_{0A}$ ,  $F_{0B}$ , show that these aggregates have small, dense cores (there are almost no empty sites in their centres, but are quite loosely packed on their periphery). This agrees with the fact that colloid growth is well pronounced in many alkali halides only at higher temperatures (e.g. at  $T \geq 60^\circ\text{C}$  in NaCl [6]).

At 500 K the aggregates are characterized by nearly the same small core but have a much larger radius  $r \approx 120a_0$ . Very large values of the joint correlation functions of similar defects,  $F_{AA}$ ,  $F_{BB} \approx 10^4$  as  $r \rightarrow 0$ , clearly demonstrate colloid formation at this temperature.

## 5. Conclusion

We presented here results of the first-principles theory of colloid formation through the aggregation of similar interacting particles during the bimolecular reaction  $A + B \rightarrow 0$  (annihilation) with the permanent particles' source and applied it successfully to the discrete-lattice description of the kinetics of the aggregation (colloid formation) in a model alkali halide crystal exposed to irradiation. We have shown that this process includes several stages: it begins with a reduction of the mobility of interstitials via their aggregation, then vacancy aggregation is triggered, and at the last stage the essentially cooperative behaviour in the aggregation of the two kinds of Frenkel defects leads to their quite similar aggregates.

## Acknowledgements

This research has been financially supported by the Volkswagen Foundation. V.K. is also indebted to the Alexander von Humboldt Foundation for financial support.

## References

- [1] P.W. Levy, J. Phys. Chem. Solids 52 (1991) 319.
- [2] W.J. Soppe, J. Prij, Nucl. Technology 107 (1994) 243.
- [3] M. Zaiser, W. Frank, A. Seeger, Sol. State Phenom. 23/24 (1992) 203.
- [4] P. Bellon, G. Martin, Sol. State Phenom. 30/31 (1993) 107.
- [5] E.R. Hodgson, A. Delgado, J.L. Alvarez Rivas, Phys. Rev. B. 18 (1978) 2911.
- [6] J.R.W. Weerkamp, J.C. Groote, J. Seinen, H.W. den Hartog, Phys. Rev. B. 50 (1994) 9781.
- [7] S.J. Zinkle, Nucl. Instr. Meth. B91 (1994) 234.
- [8] M. Cross, P.C. Holenberg, Rev. Mod. Phys. 65 (1993) 3.
- [9] W.J. Soppe, J. Phys.: Condens. Matter 5 (1993) 3519.
- [10] U. Jain, A.B. Lidiard, Phil. Mag. 35 (1977) 245.
- [11] A.B. Lidiard, Phil. Mag. A 39 (1979) 647.
- [12] E.A. Kotomin, M. Zaiser, W.J. Soppe, Phil. Mag. A 70 (1994) 313.
- [13] V.N. Kuzovkov, E.A. Kotomin, Physica Scripta 47 (1993) 585.
- [14] V.N. Kuzovkov, E.A. Kotomin, J. Chem. Phys. 98 (1993) 9107.
- [15] V.N. Kuzovkov, E.A. Kotomin, J. Stat. Phys. 72 (1993) 127.

- [16] I.M. Sokolov, A. Blumen, *Phys. Rev. E* 50 (1994) 2335.
- [17] V.N. Kuzovkov and E.A. Kotomin, 1997, to be published.
- [18] V.N. Kuzovkov, E.A. Kotomin, *Rept. Progr. Phys.* 51 (1988) 1479.
- [19] A. Kotomin, V.N. Kuzovkov, *Rept. Progr. Phys.* 55 (1992) 2079.
- [20] E.A. Kotomin, V.N. Kuzovkov, W. Frank, A. Seeger, *J. Phys. A: Gen. Math.* 27 (1994) 1453.